Science of the Total Environment 803 (2022) 149969

Contents lists available at ScienceDirect

Science of the Total Environment

journal homepage: www.elsevier.com/locate/scitotenv

Effect-directed identification of novel aryl hydrocarbon receptor-active aromatic compounds in coastal sediments collected from a highly industrialized area

Jiyun Gwak [a,1], Jihyun Cha [a,1], Junghyun Lee [b], Youngnam Kim [a], Seong-Ah An [a], Sunggyu Lee [c], Hyo-Bang Moon [c], Jin Hur [d], John P. Giesy [e,f], Seongjin Hong [a,*], Jong Seong Khim [b,*]

[a] Department of Marine Environmental Science, Chungnam National University, Daejeon 34134, Republic of Korea
[b] School of Earth and Environmental Sciences, Research Institute of Oceanography, Seoul National University, Seoul 08826, Republic of Korea
[c] Department of Marine Science and Convergence Engineering, Hanyang University, Ansan 15588, Republic of Korea
[d] Department of Environment and Energy, Sejong University, Seoul 05006, Republic of Korea
[e] Department of Veterinary Biomedical Sciences & Toxicology Centre, University of Saskatchewan, Saskatoon, SK S7N5B3, Canada
[f] Department of Environmental Science, Baylor University, Waco, TX 76798-7266, United States

HIGHLIGHTS

- Novel AhR agonists were identified in industrial sediments using EDA combined with FSA.
- 7,12DbA, 10MbA, 7MbA, and 20MC had significant AhR-mediated potencies.
- Relative potency values of novel AhR agonists compared to benzo[*a*]pyrene were obtained.
- Novel AhR agonists explained from 0.007 to 1.7% of total induced AhR potencies.

GRAPHICAL ABSTRACT

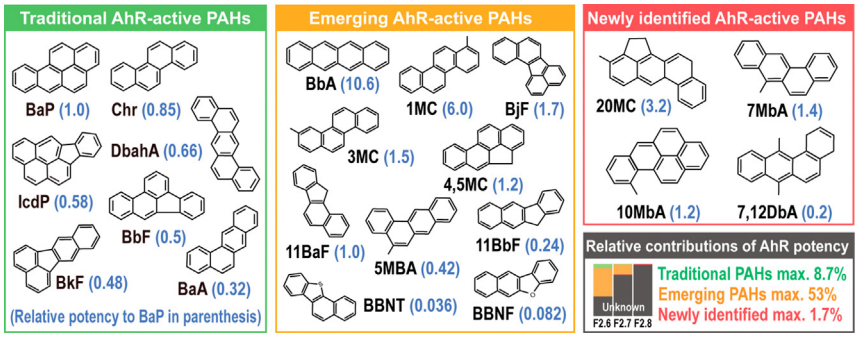

ARTICLE INFO

Article history:
Received 22 June 2021
Received in revised form 24 August 2021
Accepted 24 August 2021
Available online 28 August 2021

Editor: Shuzhen Zhang

Keywords:
Aryl hydrocarbon receptor
H4IIE-*luc* bioassay
GC-QTOFMS
Full-scan screening analysis
Industrial area

ABSTRACT

In this study, we identified major aryl hydrocarbon receptor (AhR) agonists in the sediments from Yeongil Bay (n = 6) using effect-directed analysis. Using the H4IIE-*luc* bioassays, great AhR-mediated potencies were found in aromatic fractions (F2) of sediment organic extracts from silica gel column chromatography and sub-fractions (F2.6–F2.8) from reverse phase-HPLC. Full-scan mass spectrometric analysis using GC-QTOFMS was conducted to identify novel AhR agonists in highly potent fractions, such as F2.6–F2.8 of S1 (Gumu Creek). Selection criteria for AhR-active compounds consisted of three steps, including matching factor of NIST library (≥70), aromatic structures, and the number of aromatic rings (≥4). Fifty-nine compounds were selected as tentative AhR agonist candidates, with the AhR-mediated activity being assessed for six compounds for which standard materials were available commercially. Of these compounds, 20-methylcholanthrene, 7-methylbenz[*a*]anthracene, 10-methylbenz[*a*]pyrene, and 7,12-dimethylbenz[*a*]anthracene exhibited significant AhR-mediated potency. Relative potency values of these compounds were determined relative to benzo[*a*]pyrene to be 3.2, 1.4, 1.2, and 0.2, respectively. EPA positive matrix factorization modeling indicated that the sedimentary AhR-active aromatic compounds primarily originated from coal combustion and vehicle emissions. Potency balance analysis indicated that four novel AhR agonists explained 0.007% to 1.7% of bioassay-derived AhR-mediated potencies in samples.

* Corresponding authors.
E-mail addresses: hongseongjin@cnu.ac.kr (S. Hong), jskocean@snu.ac.kr (J.S. Khim).
[1] These authors contributed equally to this work.

https://doi.org/10.1016/j.scitotenv.2021.149969
0048-9697/

1. Introduction

Instrumental analysis (targeted analysis) is an important component for assessing potential risk on aquatic organisms of environmental samples; however, this approach cannot be used to identify specific compounds that might post hazards in samples containing mixtures (Brack et al., 2016; Escher et al., 2020; Hong et al., 2015; Zhang et al., 2018). Bioassays are used to evaluate the integrated effects of chemical mixtures present in environmental samples; however, isolating and identifying specific compounds that cause effects is challenging (Brack, 2003). Effect-directed analysis (EDA) has been used as a useful tool to identify causative compounds in environmental mixture samples, including sediments, biota, and/or wastewater (Hong et al., 2016a; Simon et al., 2013; Zwart et al., 2020). The principle of EDA is first to identify highly potent fractions in extracts of environmental samples using bioassays and consecutive fractionation using open column chromatography and/or high performance liquid chromatography (HPLC). The next step is to identify causative substances in more potent fractions through targeted and nontargeted analysis. Because some toxicants in environmental samples have not been previously identified, analyzing only the targeted compounds might not fully explain the results of bioassays (An et al., 2021; Cha et al., 2019; Kim et al., 2019; Lee et al., 2017a).

Within the last decade, EDA combined with full-scan mass spectrometric analysis (FSA) has been conducted to identify unmonitored (i.e., unknown) toxicants in environmental samples (Cha et al., 2019; Kim et al., 2019; Lee et al., 2020). FSA identifies previously unidentified toxicants in samples through more sophisticated mass detection using high-resolution mass spectrometry, including gas chromatography quadrupole-time-of-flight mass spectrometry (GC-QTOFMS) (Ibáñez et al., 2008; Schymanski et al., 2015). High-resolution mass spectrometry can obtain accurate masses that have unique elemental compositions. Structures can then be elucidated based on patterns of mass fragmentation. Library matching software enhances its accuracy when searching for candidates to identity, generation, and relevance based on molecular mass matching compounds during analyses of data (Booij et al., 2014; Hollender et al., 2017; Moschet et al., 2018; Muz et al., 2017; Ouyang et al., 2017). In previous studies, several aryl hydrocarbon receptor (AhR) agonists, including benzo[*j*]fluoranthene (BjF), benz[*b*]anthracene (BbA), and enoxolone, were successfully identified in organic extracts of sediments from highly industrialized areas in South Korea using EDA (Cha et al., 2019; Kim et al., 2019; Lee et al., 2020).

AhR that responds to external chemicals, such as polycyclic aromatic hydrocarbons (PAHs), mediates toxic reactions, including mutagenicity, carcinogenicity, and developmental toxicity (Mitchell and Elferink, 2009). AhR-active compounds are used or generated as byproducts in industries, with rivers surrounding industrial complexes introducing them to coastal areas where they could accumulate in sediments (Kim et al., 2019). Previous studies indicated that aromatic compounds with 3–5 or more aromatic rings have AhR binding affinity (Louiz et al., 2008). Such aromatics are diverse, originating from the combustion of biomass, mobile sources, and diesel combustion (Kim et al., 2019). Only a few of the many aromatic toxic substances in the environments are currently being monitored, with further studies on unknown aromatic toxic substances being needed.

Yeongil Bay is located in Pohang City, which is an industrialized area and is a highly polluted area in South Korea. Inorganic and organic pollutants originating from the surrounding industrial area flow into Yeongil Bay and coastal areas via the Hyeongsan River (An et al., 2021). Previous studies reported relatively great concentrations of PAHs in sediments from Yeongil Bay and the Pohang area (Kim et al., 2014; Koh et al., 2004, 2006), with concentrations exceeding existing sediment quality guidelines of effect-range-low and -median (ERL and ERM) values of National Oceanic and Atmospheric Administration (NOAA) (Long et al., 1995), Interim Sediment Quality Guidelines (ISQG) of Canadian Council of Ministers of the Environment (CCME) (CCME, 2002), and threshold and probable effect concentrations (TEC and PEC) of Florida (Macdonald et al., 1996). In addition, AhR-mediated potencies in sediments of the Pohang area were noticeably great. Yet, knowledge remains limited about unknown AhR-active compounds in sediments, particularly aromatic toxic substances (Hong et al., 2014; Koh et al., 2004).

The present study conducted EDA to identify AhR-active aromatic compounds in sediments of an industrialized area (Pohang) of South Korea. Unmonitored AhR-active compounds present in sediment organic extracts were identified based on FSA. The relative potency values (RePs) of novel AhR agonists were estimated in comparison to benzo[*a*]pyrene (BaP). Finally, contributions of individual AhR agonists (including traditional PAHs (t-PAHs), emerging PAHs (e-PAHs), styrene oligomers (SOs), and novel aromatic AhR agonists) to total AhR-mediated potencies were calculated.

2. Materials and methods

2.1. Sample collection and preparation

Surface sediments were collected using a grab sampler in six sites, including Gumu Creek (S1, industrial area), Hyeongsan River Estuary (S2), and Yeongil Bay (S3–S6) in May 2018 (Fig. 1). Samples were transferred to pre-cleaned glass bottles and stored at −20 °C until analysis. Sediment samples were freeze-dried, sieved using 1-mm sieve, and homogenized. The organic extracts of the sediments were prepared using a Soxhlet extractor and were used for bioassays, chemical analyses, and further fractionations (Hong et al., 2016a). Forty grams of the sediment samples were extracted on a Soxhlet apparatus with methylene chloride (Burdick and Jackson, Muskegon, MI). After removing elemental sulfur in organic extracts using activated Cu, the extracts were concentrated to 4 mL (10 g sediment equivalent (SEq) mL^{-1}) using a rotary evaporator and nitrogen gas concentrator. Raw extracts (REs) were divided into two aliquots (3 and 1 mL) for further fractionations and bioassays, respectively. The solvent of REs for bioassay was exchanged to dimethyl sulfoxide (Sigma-Aldrich, St. Louis, MO).

2.2. Silica gel and RP-HPLC fractionations

REs were fractionated through silica gel column chromatography and reverse-phase HPLC (details in Hong et al., 2015, 2016b). Briefly, 8 g of silica gel (70–230 mesh, activated, Sigma-Aldrich) was packed into a column (30 cm long × 1 cm i.d.) with hexane. Three milliliters of organic extract were separated into aliphatics (F1), aromatics (F2), and polar (F3) fractions. F1, F2, and F3 were eluted with 30 mL of hexane, 60 mL of 20% methylene chloride in hexane, and 50 mL of 40% acetone in methylene chloride, respectively. In the second step, F2 was separated into ten subfractions using RP-HPLC (Agilent 1260 HPLC, Agilent Technologies, Santa Clara, CA) with a ZORBAX Eclipse PrepHT XBD-C18 column (250 mm × 21.2 mm, 7 μm, Agilent). Detailed information on instrumental conditions of RP-HPLC, including sampling volume, sampling time, and log K_{OW} intervals, are presented in Table S1 of the Supplementary Materials (Hong et al., 2016b). The solvent of fraction samples was exchanged to hexane or dimethyl sulfoxide for targeted and nontargeted analyses and bioassays, respectively.

2.3. H4IIE-luc transactivation bioassays

AhR-mediated potencies were measured using the H4IIE-*luc* bioassay in REs and fraction samples (Hong et al., 2016b). Trypsinized cells were diluted to approximately 7.0×10^4 cells mL^{-1} and seeded into the 60 interior wells of 96 well micro-plates at 250 μL $well^{-1}$ (Details in Table S2). After incubation overnight at 37 °C in a 5% CO_2, test and control wells were dosed with the appropriate standards (positive control, BaP), sample extracts (REs, fractions, and AhR

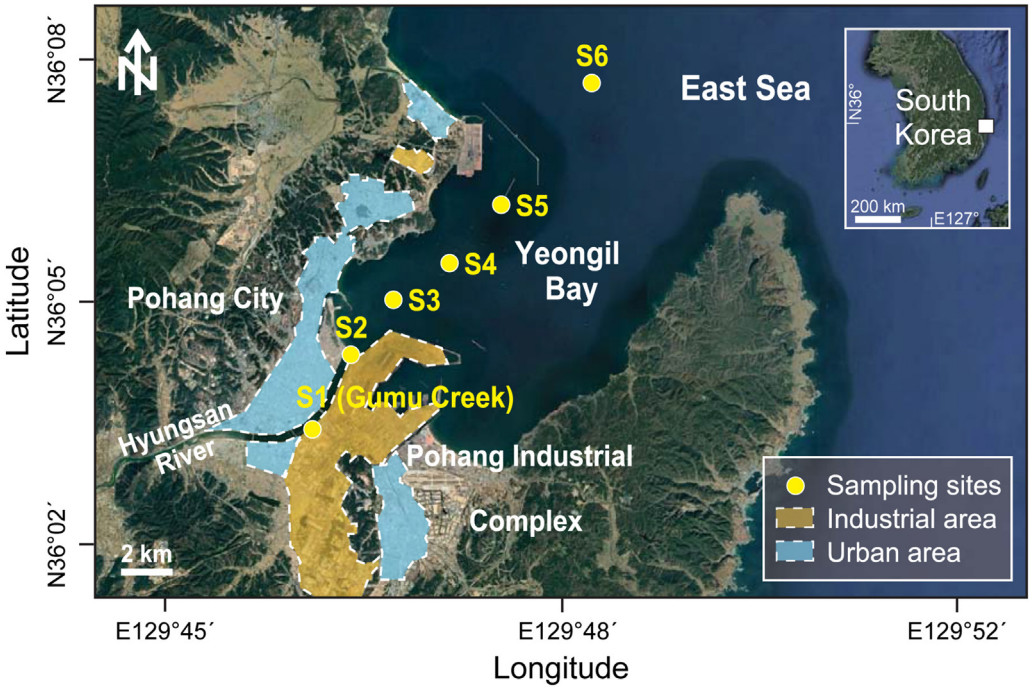

Fig. 1. Sampling sites of surface sediments from Yeongil Bay, South Korea.

agonist candidates), or solvent controls (0.1% DMSO). Luciferase assays were conducted after 4 h exposure using a multi-label plate reader (Victor X3, PerkinElmer, Waltham, MA). Responses of bioassay expressed as mean relative luminescence units (RLUs) were converted to percentages of maximum response of BaP (%BaP_{max}) observed for 50 nM (=100%BaP_{max}). Potency-based BaP-equivalent (EQ) concentrations (ng BaP-EQ g^{-1} dm) were calculated from dose-response curves of the samples at six concentrations. All bioassays were conducted in triplicate to check the reproducibility.

2.4. Targeted chemical analysis

Forty-four target compounds, including 15 t-PAHs, 19 e-PAHs, and 10 SOs, were analyzed in fraction samples following previous studies (Kim et al., 2019). Instrumental conditions of GC-MSD (Agilent 7890B GC and 5977A MSD, Agilent Technologies) and the full name of target compounds are presented in Tables S3 and S4, respectively. The sedimentary concentrations of t-PAHs and SOs were partially reported in a previous study (An et al., 2021). Rates of recovery of deuterated surrogate standards (acenaphthene-*d*10, phenanthrene-*d*10, chrysene-*d*12, and perylene-*d*12) were measured to determine whether compounds loss occurs during experiments. The average recovery of surrogate standards for PAHs were 100% for acenaphthene-*d*10 (89–110%), 93% for phenanthrene-*d*10 (86–99%), 87% for chrysene-*d*12 (82–89%) and 71% for perylene-*d*12 (58–83%) (An et al., 2021). Method detection limits (MDL, standard deviation × 3.707 of the lowest calibration standard) for t-PAHs, e-PAHs, and SOs range from 1.1–12 ng g^{-1} dm, 0.06–-6.8 ng g^{-1} dm, and 0.11–0.89 ng g^{-1} dm, respectively. More information on QA/QC is provided in Table S4.

2.5. Nontargeted analysis

FSA was conducted on highly potent HPLC fractions, such as F2.6–F2.8 of S1 using GC-QTOFMS. Detailed instrumental settings are provided in Table S5. The tentative candidates for AhR agonists were selected through three-step criteria. At first, the compounds with more than 70 of matching scores in the NIST library (Version 2014) were selected (Zedda and Zwiener, 2012). The second step involved identifying compounds, which had aromatic rings. The third step selected the compounds with four or more aromatic rings. Finally, six tentative AhR agonists were selected, including 7,12-dimethylbenz[*a*]anthracene (7,12DbA), 7-methylbenz[*a*]anthracene (7MbA), 10-methylbenz[*a*]pyrene (10MbA), 20-methylcholanthrene (20MC), dibenzo[*e*,*l*]pyrene (DeP), and benzo[*b*]naphthacene (BbN). The standard materials of these compounds were obtained from Sigma-Aldrich. The six tentative AhR agonists were subjected to chemical and toxicological confirmation.

2.6. Relative potency values of novel AhR agonists

ReP values compared to BaP were estimated for compounds showing significant AhR-mediated potencies among six candidate compounds. Each compound was diluted serially at the six concentrations (10,000, 3333, 1111, 370, 120, and 41 ng mL^{-1}), and was measured for AhR-mediated potencies (Horii et al., 2009a; Villeneuve et al., 2000). ReP values of the compounds were based on median effective concentrations (EC50), and were calculated as ratios with the EC50 of BaP in the H4IIE-*luc* bioassay.

2.7. Potency balance analysis

AhR-mediated potencies measured between instrumental analysis (BaP equivalent concentrations, BEQs) and bioassays (BaP-EQs) were directly compared to determine contributions of individual AhR agonists to total induced potencies. Concentrations of BEQ were obtained from the sum of concentrations of target compounds multiplied by their assay-specific RePs (Koh et al., 2004; Villeneuve et al., 2000). Assay-specific ReP values of t-PAHs, e-PAHs, and SOs are presented in Table S6. ReP values of novel AhR agonists obtained in the present study were used.

2.8. Positive matrix factorization receptor model

The US EPA positive matrix factorization (PMF, Version 5.0) model was used for the identification of sources of PAHs in sediments. Input datasets were 15 t-PAHs × 6 sites. The 2-factor solution was selected

due to showing the most reliable results with the smallest value of Q_{True}/Q_{Exp}. The slope in the linear regression ranged from 0.39 to 1.31, with an R^2 value of 0.99. It is indicated that the results of the PMF model in the present study were satisfactory.

2.9. In silico modeling using VEGA QSAR and VirtualToxLab

The 59 tentative AhR agonist candidates identified by FSA were estimated using VirtualToxLab, to confirm binding affinity with AhR. VirtualToxLab, a quantitative structure-activity relationship (QSAR) modeling approach, could be used to quantify and simulate toxic potentials of chemicals for various endpoints (Marzo et al., 2016; Vedani et al., 2015). In addition, for the six candidate compounds, estrogenic activity, mutagenicity, carcinogenicity, and developmental toxicity potentials were evaluated using VEGA-QSAR (Pizzo et al., 2013).

3. Results and discussion

3.1. AhR-mediated potencies in raw extracts and fractions

All REs of sediments reached saturation efficacy (≥100%BaP_{max}) for AhR-mediated potencies (Fig. 2a). Among the silica gel fractions, F2 (aromatics) and F3 (polar) exhibited great AhR-mediated potencies in S1 and S2 sediments (Fig. 2b). Great AhR-mediated potencies in F2 and F3 were also observed in previous studies conducted in highly industrialized areas, including Lake Sihwa (Cha et al., 2019; Lee et al., 2017b) and Ulsan Bay (Kim et al., 2019), South Korea. This phenomenon was attributed to certain compounds able to bind with AhR, including PAHs, existing in F2 of sediment extracts (Kinani et al., 2010). The present study supports the results of previous studies, which detected great PAH concentrations in the sediments of Yeongil Bay (An et al., 2021; Hong et al., 2014; Koh et al., 2004). In the current study, additional steps were applied to identify AhR agonists focusing on the aromatic compounds in sediment extracts.

F2 of S1 and S2 were fractionated into ten fine fractions using RP-HPLC, and AhR-mediated potencies were also evaluated. Among the ten subfractions, significant AhR-mediated potencies were detected in F2.6, F2.7, and F2.8 of S1 and S2 (Fig. 2c). These fractions contained aromatic compounds with log K_{OW} values of 5–6, 6–7, and 7–8, respectively. Known AhR agonists (including benzo[*a*]anthracene (BaA), BbA, chrysene (Chr), 1,3-diphenylpropane (SD1), and 2,4-diphenyl-1-butene (SD3)) occurred in F2.6, while benzo[*b*]fluoranthene (BbF), benzo[*k*]fluoranthene (BkF), BaP, BjF, Indeno[*1,2,3-cd*]pyrene, dibenz[*a,h*]anthracene, and 1e-phenyl-4e-(1-phenylethyl)-tetralin occurred in F2.7 (Cha et al., 2019; Kim et al., 2019). Greater AhR-mediated potencies were frequently detected in F2.6–F2.8 by previous studies conducted on the sediments of other industrialized areas, including Ulsan Bay (Kim et al., 2019), Lake Sihwa (Cha et al., 2019; Hong et al., 2016b), and Masan Bay (Lee et al., 2020) in South Korea.

EC50 values of highly potent fractions (F2.6–F2.8 of S1 and S2) were calculated from the dose-response curves (Fig. 2d). S1 had relatively greater AhR-mediated potencies (11,000–190,000 ng BaP-EQ g^{-1} dm) compared to S2 (330–1000 ng BaP-EQ g^{-1} dm). In the current study, AhR-mediated potencies in the sediments (BaP-EQs) of Yeongil Bay were greater than those of Ulsan Bay (190–12,000 ng BaP-EQ g^{-1} dm) (Kim et al., 2019) and Lake Sihwa (7.5–15,000 ng BaP-EQ g^{-1} dm) (Cha et al., 2019). Meanwhile, mixture toxic effects between fractions were not considered in the present study. AhR-mediated potency in each fraction (F2.6–F2.8) was directly compared with potencies of aromatic AhR agonists present in the fraction. Potency balance analyses, based on RePs of AhR agonists, basically assume that AhR-mediated potency by each AhR agonist is additive. In several previous studies using H4IIE-*luc* bioassays, it was confirmed that the mixture of PAHs exhibited AhR-mediated potencies additively (Larsson et al., 2012, 2014).

3.2. Concentrations and toxicity contributions of target AhR-active compounds

Target AhR-active compounds (t-PAHs, e-PAHs, and SOs) were detected in F2.6 and F2.7 fractions of S1 and S2 (Fig. 3a and Table S7). Concentrations of AhR-active compounds in S1 and S2 sediments were 93,000 ng g^{-1} dm and 240 ng g^{-1} dm, respectively (Fig. 3a). Concentrations of these compounds were greater in S1 because they mainly originated from industrial complexes. In F2.6 of S1, benzo[*b*]naphtho[*2,3-d*]furan (BBNF) was detected at great concentrations, followed by BaA, Chr, BbA, SD3, and SD1. For F2.6 of S2, SD3 had the greatest concentrations, followed by BbA, BaA, Chr, SD1, and BBNF. Greater concentrations

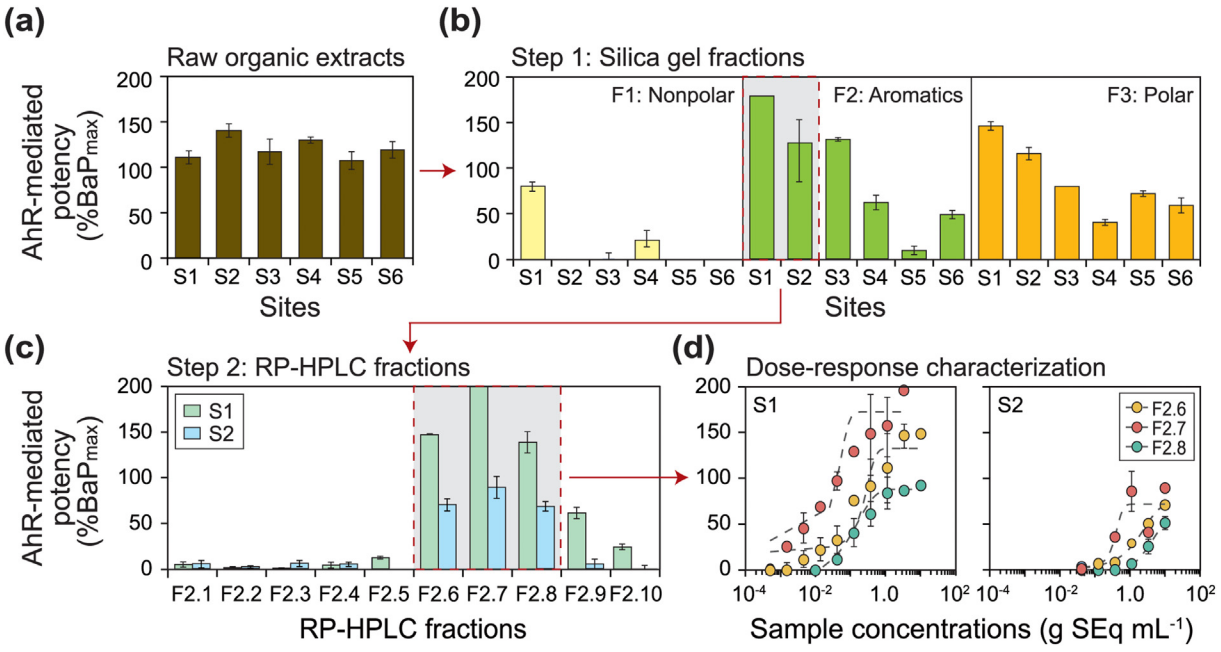

Fig. 2. AhR-mediated potencies of (a) raw extracts, (b) silica gel fractions, and (c) RP-HPLC fine fractions of sediments from Yeongil Bay. (d) Dose-response curves for AhR-mediated potencies of selected RP-HPLC fractions (F2.6–F2.8 of S1 and S2) (error bar: mean ± SD, $n = 3$).

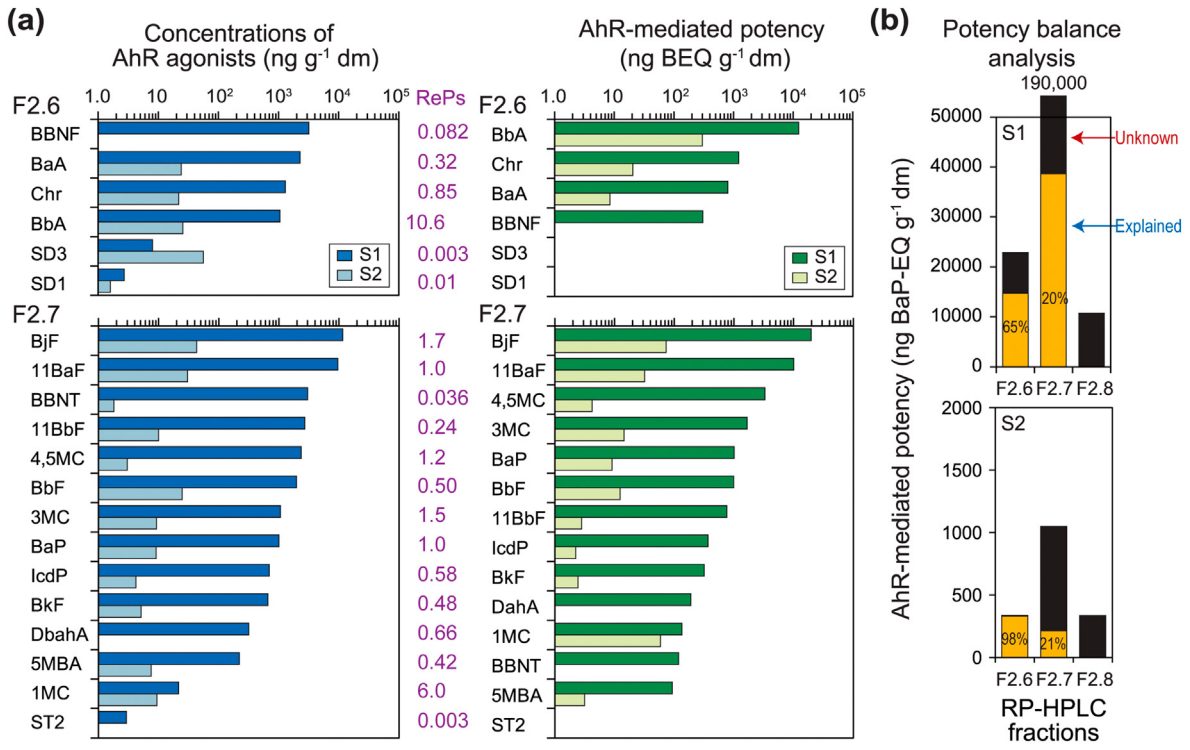

Fig. 3. (a) Concentrations and instrument-derived BEQs of AhR-active compounds in F2.6 and F2.7 of S1 and S2 and (b) contribution of targeted PAHs and SOs to BaP-EQs (potency based).

of BjF and 11H-benzo[*a*]fluorene (11BaF) were commonly found in F2.7 of S1 and S2 sediments.

Concentrations of instrument-derived BEQs of target compounds in F2.6 were ordered as BbA, Chr, BaA, BBNF, SD1, and SD3, both S1 and S2. BbA had the greatest RePs and concentrations in sediments. Thus, BbA contributed the most to total BEQ concentrations. The BEQs of BjF and 11BaF also contributed the most to F2.7, due to high concentrations in sediments. BbA and BjF mainly originated from OLED film and coal combustion, respectively (Gundlach et al., 2002; Kim et al., 2019; Takahashi et al., 2007). SOs contributed less to total BEQs, due to lesser concentrations and RePs.

Potency balance analysis determined the contributions of target AhR agonists in fraction samples between instrument-derived BEQs and bioassay-derived BaP-EQs (Fig. 3b). Potency balance analysis was conducted on F2.6 and F2.7 of S1 and S2. Analysis of F2.8 was not possible because there was no target compound. Known AhR-active compounds explained moderate portions of the bioassay-derived BaP-EQs based on potency balance analysis. The instrument-derived BEQs of F2.6 showed 65% and 98% of bioassay-derived BaP-EQs, while the BEQs of F2.7 showed a lower contribution (20% and 21%) of BaP-EQs. Overall, previously unidentified AhR-active compounds were noticeably present in F2.6–F2.8 of S1; thus, FSA was performed using GC-QTOFMS.

3.3. Identification of unknown AhR agonists in fractions

Candidates for AhR agonists in F2.6–F2.8 of S1 were narrowed, following three steps (Fig. 4a). In the first step, 321, 425, and 240 compounds were matched with the NIST library in F2.6, F2.7, and F2.8 of S1, respectively. To identify chemicals accurately, the matching score was 70 or greater. Consequently, 229, 278, and 171 compounds were selected in each fraction (F2.6–F2.8). In the second step, aromatic compounds were selected. Results of previous studies showed that the planar structure of aromatic compounds (e.g., polychlorinated dibenzo-*p*-dioxins and dibenzofurans, coplanar polychlorinated biphenyls, and PAHs) tends to bind to AhR (Mekenyan et al., 1996). In the present study, 110, 151, and 71 compounds remained in F2.6, F2.7, and F2.8, respectively. Finally, when compounds with four or more aromatic rings were selected, 10, 36, and 13 compounds represented tentative candidates for AhR agonists in F2.6–F2.8 (Table S8). These compounds were mainly identified as i) 200–400 molecular mass, ii) retention time 20–30 min, and iii) log K_{OW} 5–8 compounds (Fig. 4a). Finally, based on a three-step set of criteria, fifty-nine compounds were selected as AhR agonist candidates in S1 sediment (Table S8). Of these, only six compounds were commercially available as standard materials (specifically 7,12DbA, 7MbA, 10MbA, 20MC, BbN, and DeP), and toxicological and chemical confirmation was performed.

3.4. Toxicological and chemical confirmation

Toxicological and chemical confirmation for the six AhR agonist candidates were conducted to assess AhR binding potencies and to quantify concentrations in sediments. Among the six candidates, four compounds exhibited significant AhR-mediated potencies, namely, 7,12DbA, 10MbA, 7MbA, and 20MC (Fig. 4b). ReP values for individual compounds were newly obtained in the present study. In the previous study, it was reported that EC50 values could be used when maximum responses of compounds are more than half that of the reference standard (Bols et al., 1999). Variation among ReP_{20}, ReP_{50}, and ReP_{80} was relatively small (within an order of magnitude); thus, the use of ReP_{50} was considered reliable (Horii et al., 2009b; Villeneuve et al., 2000) (Table S9). ReP values of 7,12DbA, 7MbA, 10MbA, and 20MC compared to BaP were 0.2, 1.4, 1.2, and 3.2, respectively (Fig. 4b). Three newly identified AhR agonists (except for 7,12DbA) had greater AhR binding potencies compared to BaP, which is a representative AhR-active compound. In particular, 20MC had three times greater AhR binding affinity compared to BaP, which was previously reported to act as an AhR agonist (Shipley and Waxman, 2006). The present study provided the first report of AhR binding affinity for 7,12DbA, 10MbA, and 7MbA. GC retention time and ion fragment patterns of novel AhR-active PAHs (n-PAHs) were confirmed using standard

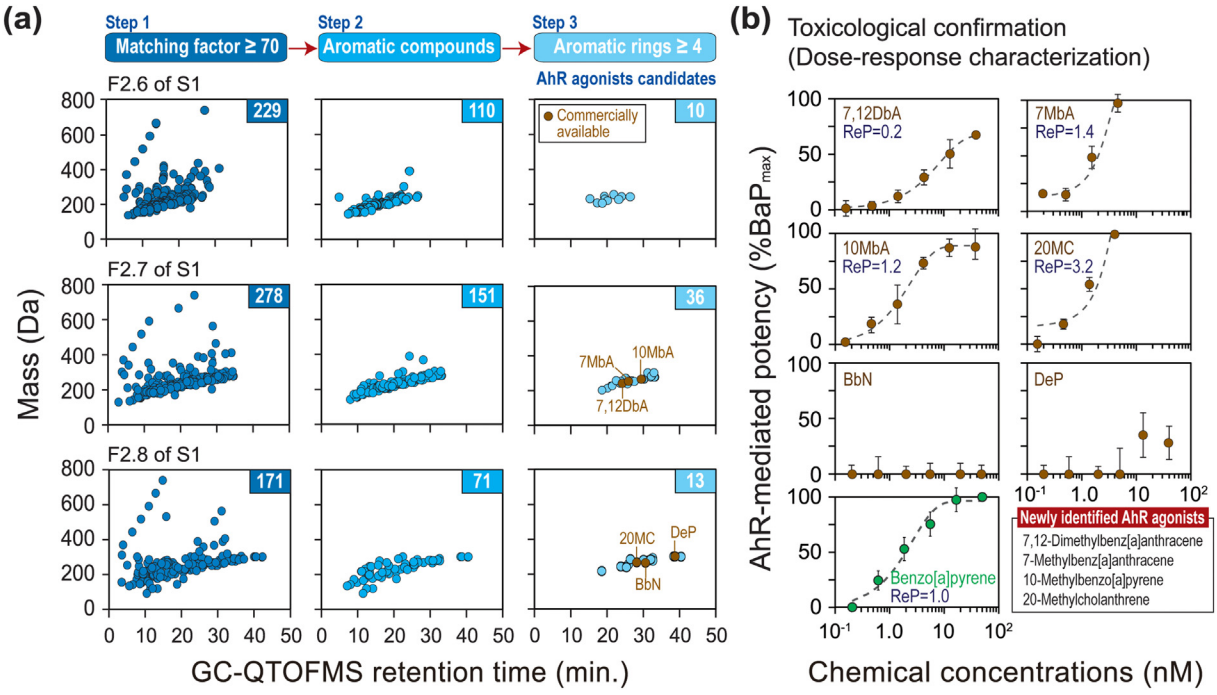

Fig. 4. (a) Three-step selection processes of GC-QTOFMS data analysis for potential AhR agonists and (b) dose-response curves for AhR-mediate potencies of six candidates of AhR agonists and benzo[*a*]pyrene in the H4IIE-*luc* bioassay (error bar: mean ± SD, $n = 3$).

materials (Table S10). Concentrations of n-PAHs in sediments were quantified using GC-MSD.

3.5. Distributions of novel AhR-active compounds in sediments

S1 contained the greatest concentrations of n-PAHs, followed by S2, S4, S5, S6, and S3 (Fig. 5a). Concentrations of 10MbA, 7,12BaA, 7MbA, and 20MC in S1 were 500 ng g^{-1} dm, 430 ng g^{-1} dm, 80 ng g^{-1} dm, and 60 ng g^{-1} dm, respectively. The spatial distribution pattern of n-PAHs was similar to that of t-PAHs, e-PAHs, and SOs (Fig. S1). Thus, these n-PAHs likely originated from the surrounding industrial complexes, similar to other organic toxic substances, and accumulated in sediments (Hong et al., 2014). Previous studies reported that 10MbA originates from coal combustion and vehicle emissions (Venkataraman et al., 1994). There are no previous reports on the sources of 7,12BaA, 7MbA, and 20MC.

The EPA PMF model was used to identify the potential source of t-PAHs in the sediments of Yeongil Bay (Fig. S2a). BaA (94%), anthracene (94%), BkF(93%), and BbF (86%) were the main components of Factor 1, and likely originated from coal combustion (Kong et al., 2012; Yang et al., 2013; Zhang et al., 2019). Phenanthrene (70%), fluorene (38%), and acenaphthene (37%) were the main components of Factor 2, and likely originated from vehicle emissions (Ravindra et al., 2008; Yang et al., 2013; Zhang et al., 2012, 2019). Factor 1 and Factor 2 had the greatest contribution of S1 sediments (Fig. S2b). Most coal combustion and vehicle emissions of sedimentary PAHs in Yeongil Bay were explained by nearby sources. n-PAHs are likely to originate from similar sources of t-PAHs in Yeongil Bay.

3.6. Contribution of target compounds to total induced AhR-mediated potencies

Potency balance analysis showed that n-PAHs explained only a small portion of BaP-EQs (Table 1 and Fig. 5b). Although 10MbA and 7MbA had greater ReP values, the contribution was 0.42% and 0.63% of total AhR-mediated potencies, respectively. This phenomenon was attributed to the relatively low concentrations of these chemicals in the sediments of Yeongil Bay. 7,12DbA contributed 0.04% (S1) and 0.007% (S2)

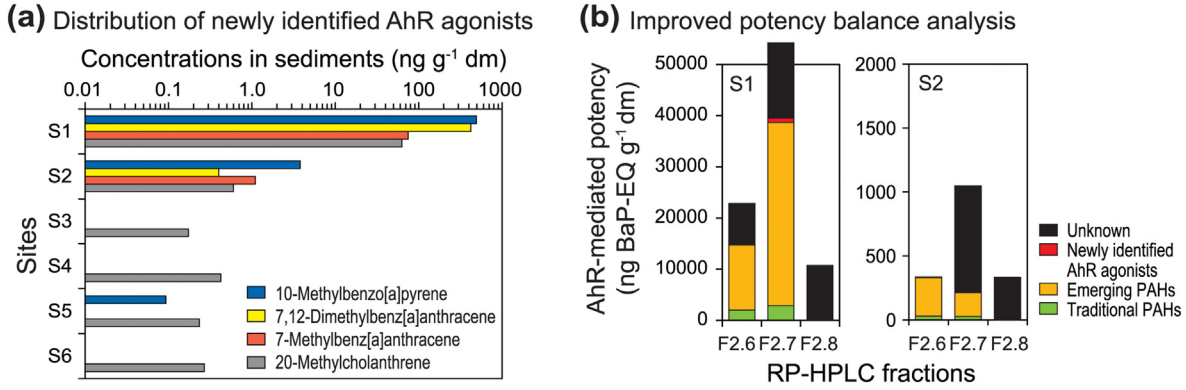

Fig. 5. (a) Distributions of novel AhR-active compounds in the sediments of Yeongil Bay, South Korea. (b) Contribution of individual AhR agonists, including novel AhR agonists to BaP-EQs. (F2.6–F2.8 of S1 and S2).

Table 1
Potency balance between instrument-derived BEQs and bioassay-derived BaP-EQs in the RP-HPLC fractions (F2.6, F2.7, and F2.8 of S1 and S2) of the sediments in Yeongil Bay, South Korea.

Compound	Abb[a]	Site 1			Site 2		
		F2.6	F2.7	F2.8	F2.6	F2.7	F2.8
Instrument-derived BEQs (ng BEQ g^{-1} dm)							
Traditional PAHs and SOs							
Benz[*a*]anthracene	BaA	800			8.5		
Chrysene	Chr	1200			20		
1,3-Diphenylpropane	SD1	0.01			0.005		
2,4-Diphenyl-1-butene	SD3	0.003			0.02		
Benzo[*b*]fluoranthene	BbF		990			12	
Benzo[*k*]fluoranthene	BkF		300			2.5	
Benzo[*a*]pyrene	BaP		1000			9.1	
Indeno[*1,2,3-c,d*]pyrene	IcdP		370			2.2	
Dibenz[*a,h*]anthracene	DahA		190				
2,4,6-Triphenyl-1-hexene	ST2		0.01				
Emerging PAHs							
Benzo[*b*]naphtho[*2,3-d*]furan	BBNF	300					
Benz[*b*]anthracene	BbA	12,000			300		
11H-Benzo[*b*]fluorine	11BbF		760			2.8	
Benzo[*b*]naphtho[*2,1-d*]thiophene	BBNT		120			0.07	
3-Methylchrysene	3MC		1700			14	
5-Methylbenz[*a*]anthracene	5MBA		93			3.2	
1-Methylchrysene	1MC		130			59	
Benzo[*j*]fluoranthene	BjF		20,000			73	
11H-Benzo[*a*]fluorine	11BaF		10,000			32	
4,5-Methanochrysene	4,5MC		3300			4.2	
Newly identified AhR agonists							
10-Methylbenzo[*a*]pyrene	10MbA		580			0.1	
7,12-Dimethylbenz[*a*]anthracene	7,12DbA		79			4.91	
7-Methylbenz[*a*]anthracene	7MbA		170			1.7	
20-Methylcholanthrene	20MC			190			2.0
Bioassay-derived BaP-EQs (ng BaP-EQ g^{-1} dm)		2.3×10^4	1.9×10^5	1.1×10^4	3.4×10^2	1.0×10^3	3.3×10^2
Contribution (%)		65	20	1.7	98	21	0.6

[a] Abb.: abbreviations.

to BaP-EQs of F2.7, due to small ReP values. 20MC was identified in F2.8 for the first time and contributed to BaP-EQ in S1 (1.7%) and S2 (0.6%). VirtualToxLab was performed to assess the AhR binding affinity for 59 tentative AhR agonists (Table S8). Several compounds had higher AhR binding affinity compared to the four n-PAHs. Since these candidates have the potential to conspicuously contribute to the total induced AhR-mediated potencies, further toxicological confirmation is required.

The relative contributions of AhR-active compounds in sediments conducted in Ulsan Bay, Lake Sihwa, Masan Bay, and Yeongil Bay were compared (Table S11). The AhR-active PAHs, including t-PAHs and e-PAHs, were widely distributed in coastal sediments near industrial areas. Contributions of AhR agonists varied greatly among regions. Toxicity varied depending on the type of surrounding industries. AhR agonists with the highest contributions were detected in a region-specific

Table 2
Predicted potential toxic effects of six candidates of AhR-active compounds in sediments in Yeongil Bay, South Korea, using VEGA QSARs and VirtualToxLab modeling.

Compound	Reported toxicity (References)	Predicted potential toxicity				AhR binding affinity	
		Estrogenic activity[a]	Mutagenicity[b]	Carcinogenicity[c]	Developmental toxicity[d]	H4IIE-*luc* bioassay	VirtualToxLab modeling
F2.7							
7,12-Dimethylbenz[*a*]anthracene	n.a[e]	+[f]–[g]	+ + + + +	+ + + +	+ −	+	Low binding (654 nm)
10-Methylbenz[*a*]pyrene	n.a	+ −	+ + + + +	+ + + +	+ −	+	Low binding (521 nm)
7-Methylbenz[*a*]anthracene	Mutagenicity (Cerniglia et al., 1982) Tumorigenicity (Cerniglia et al., 1982)	+ −	+ + + + +	+ + + +	+ −	+	Moderate binding (461 nm)
F2.8							
20-Methylcholanthrene	AhR activity (Shipley and Waxman, 2006)	+ −	+ + + + +	+ + + +	+ −	+	Moderate binding (195 nm)
Dibenzo[*e,l*]pyrene	Carcinogenicity (Yu and Campiglia, 2005)	+ −	+ + + + +	− + − +	− +		Moderate binding (201 nm)
Benzo[*b*]naphthacene	n.a	+ −	+ + + + +	− + − +	− +	−	n.a

[a] Predicted using IRFMN and IRFMN/CERAPP models.
[b] Predicted using CAESAR, ISS, CONSENSUS, KNN/Read-Across, and SarPY/IRFMN models.
[c] Predicted using CAESAR, ISS, IRFMN/Antares, and IRFMN/ISSCAN-CGX models.
[d] Predicted using CAESAR and PG models.
[e] n.a: not available.
[f] +: active.
[g] −: non-active.

manner (BjF in Ulsan Bay, BaA in Masan Bay, BbA in Lake Sihwa and Yeongil Bay). In general, the contribution of e-PAHs to total AhR-mediated potencies in sediments was greater compared to that of t-PAHs. Thus, further studies on e-PAHs are needed in the future.

3.7. Additional toxicity screening based on QSAR modeling

Previous studies reported the potential toxicities of the six AhR-active candidates (Table 2). For example, 20MC binds to the ER and AhR (Shipley and Waxman, 2006). 7MbA exhibited mutagenicity and tumorigenicity (Cerniglia et al., 1982), while DeP was classified as a carcinogen (Yu and Campiglia, 2005). To assess the additional potential toxicity of the AhR-active candidates, such as estrogenic activity, mutagenicity, carcinogenicity, and developmental toxicity potentials, VEGA QSAR was conducted (Table 2). 7,12DbA, 10MbA, 20MC, and 7MbA exhibited mutagenicity, carcinogenicity, and developmental toxicity. Furthermore, BbN and DeP exhibited mutagenicity. Overall, these compounds were mainly derived from industrial complexes and had the potential to induce other toxicities. Thus, further investigations are required.

4. Conclusions

EDA was successfully performed to determine AhR-active aromatic compounds in sediments of Yeongil Bay. Potency balance analysis showed that the contributions of e-PAHs in bioassay-derived BaP-EQs were greater compared to those of t-PAHs. When the EDA studies on the major AhR agonists in coastal sediments near the industrial complexes of Korea, the causative substances were found to be region-specific, and it seems to be associated with types of industries in the surrounding areas. Although recent studies on e-PAHs reported their distributions and potential risks to the environment, there are still not many investigations. e-PAHs mainly originate from industrial complexes and accumulate in nearby coastal sediments. AhR-mediated activity and other potential toxicity might also exist in coastal ecosystems, and many unknown toxic substances have yet to be identified. EDA combined with FSA is very effective in identifying unknown compounds that cause toxic effects in environmental samples, and such studies need to be continued in the future.

CRediT authorship contribution statement

Jiyun Gwak: Conceptualization, Investigation, Formal analysis, Data curation, Visualization, Writing - original draft.

Jihyun Cha: Conceptualization, Investigation, Formal analysis, Data curation, Writing - original draft.

Junghyun Lee: Investigation, Formal analysis, Data curation, Writing - review & editing.

Youngnam Kim: Investigation, Formal analysis.

Seong-Ah An: Investigation, Formal analysis.

Sunggyu Lee: Investigation, Formal analysis, Data curation.

Hyo-Bang Moon: Writing - review & editing, Project administration.

Jin Hur: Writing - review & editing, Project administration.

John P. Giesy: Conceptualization, Methods development, Training, Writing - review & editing.

Seongjin Hong: Conceptualization, Methods development, Writing - original draft, Writing - review & editing, Project administration, Funding acquisition, Supervision.

Jong Seong Khim: Conceptualization, Methods development, Writing - review & editing, Project administration, Funding acquisition, Supervision.

Declaration of competing interest

The authors declare that they have no known competing financial interests or personal relationships that could have appeared to influence the work reported in this paper.

Acknowledgments

This study was supported by grants from the National Research Foundation of Korea (2016R1E1A1A01943004, 2020R1A4A2002823, and 2021R1C1C1005977) and the Ministry of Oceans and Fisheries of Korea (20140342 and 20210427). Prof. John P. Giesy was supported by the Canada Research Chair program and a distinguished visiting professorship program of Baylor University.

Appendix A. Supplementary data

Supplementary data to this article can be found online at https://doi.org/10.1016/j.scitotenv.2021.149969.

References

An, S.-A., Hong, S., Lee, J., Cha, J., Lee, S., Moon, H.B., Giesy, J.P., Khim, J.S., 2021. Identification of potential toxicants in sediments from an industrialized area in Pohang, South Korea: application of a cell viability assay of microalgae using flow cytometry. J. Hazard. Mater. 405, 124230. https://doi.org/10.1016/j.jhazmat.2020.124230.

Bols, N.C., Schirmer, K., Joyce, E.M., Dixon, D.G., Greenberg, B.M., Whyte, J.J., 1999. Ability of polycyclic aromatic hydrocarbons to induce 7-ethoxyresorufin-o-deethylase activity in a trout liver cell line. Ecotox. Environ. Safe. 44 (1), 118–128. https://doi.org/10.1006/eesa.1999.1808.

Booij, P., Vethaak, A.D., Leonards, P.E., Sjollema, S.B., Kool, J., de Voogt, P., Lamoree, M.H., 2014. Identification of photosynthesis inhibitors of pelagic marine algae using 96-well plate microfractionation for enhanced throughput in effect-directed analysis. Environ. Sci. Technol. 48, 8003–8011. https://doi.org/10.1021/es405428t.

Brack, W., 2003. Effect-directed analysis: a promising tool for the identification of organic toxicants in complex mixtures? Anal. Bioanal. Chem. 377, 397–407. https://doi.org/10.1007/s00216-003-2139-z.

Brack, W., Ait-Aissa, S., Burgess, R.M., Busch, W., Creusot, N., Di Paolo, C., Escher, B.I., Mark Hewitt, L., Hilscherová, K., Hollender, J., Hollert, H., Jonker, W., Kool, J., Lamoree, M., Muschket, M., Neumann, S., Rostkowski, P., Ruttkies, C., Schollee, J., Schymanski, E.L., Schulze, T., Seiler, T.-B., Tindall, A.J., De Aragão Umbuzeiro, G., Vrana, B., Krauss, M., 2016. Effect-directed analysis supporting monitoring of aquatic environments — an in-depth overview. Sci. Total Environ. 544, 1073–1118. https://doi.org/10.1016/j.scitotenv.2015.11.102.

Canadian Council of Ministers of the Environment (CCME), 2002. Canadian sediment quality guidelines for the protection of aquatic life summary tables. CCME, Winnipeg, MB http://ceqgrcqe.ccme.ca/download/en/242?redir=1569847235.

Cerniglia, C.E., Fu, P.P., Yang, S.K., 1982. Metabolism of 7-methylbenz[a]anthracene and 7-hydroxymethylbenz[a]anthracene by Cunninghamella elegans. Appl. Environ. Microbiol. 44, 682–699. https://doi.org/10.1128/AEM.44.3.682-689.1982.

Cha, J., Hong, S., Kim, J., Lee, J., Yoon, S.J., Lee, S., Moon, H.B., Shin, K.H., Hur, J., Giesy, J.P., Khim, J.S., 2019. Major AhR-active chemicals in sediments of Lake Sihwa, South Korea: application of effect-directed analysis combined with full-scan screening analysis. Environ. Int. 133, 105199. https://doi.org/10.1016/j.envint.2019.105199.

Escher, B.I., Stapleton, H.M., Schymanski, E.L., 2020. Tracking complex mixtures of chemicals in our changing environment. Science 367, 388–392. https://doi.org/10.1126/science.aay6636.

Gundlach, D.J., Nichols, J.A., Zhou, L., Jackson, T.N., 2002. Thin-film transistors based on well-ordered thermally evaporated naphthacene films. Appl. Phys. Lett. 80, 2925–2927. https://doi.org/10.1063/1.1471378.

Hollender, J., Schymanski, E.L., Singer, H.P., Ferguson, P.L., 2017. Nontarget screening with high resolution mass spectrometry in the environment: ready to go? Environ. Sci. Technol. 51, 11505–11512. https://doi.org/10.1021/acs.est.7b02184.

Hong, S., Khim, J.S., Park, J., Kim, S., Lee, S., Choi, K., Kim, C.S., Choi, S.D., Park, J., Ryu, J., Jones, P.D., Giesy, J.P., 2014. Instrumental and bioanalytical measures of dioxin-like compounds and activities in sediments of the Pohang Area, Korea. Sci. Total Environ. 470–471, 1517–1525. https://doi.org/10.1016/j.scitotenv.2013.06.112.

Hong, S., Lee, S., Choi, K., Kim, G.B., Ha, S.Y., Kwon, B.O., Ryu, J., Yim, U.H., Shim, W.J., Jung, J., Giesy, J.P., Khim, J.S., 2015. Effect-directed analysis and mixture effects of AhR-active PAHs in crude oil and coastal sediments contaminated by the Hebei Spirit oil spill. Environ. Pollut. 199, 110–118. https://doi.org/10.1016/j.envpol.2015.01.009.

Hong, S., Yim, U.H., Ha, S.Y., Shim, W.J., Jeon, S., Lee, S., Kim, C., Choi, K., Jung, J., Giesy, J.P., Khim, J.S., 2016a. Bioaccessibility of AhR-active PAHs in sediments contaminated by the Hebei Spirit oil spill: application of tenax extraction in effect-directed analysis. Chemosphere 144, 706–712. https://doi.org/10.1016/j.chemosphere.2015.09.043.

Hong, S., Lee, J., Lee, C., Yoon, S.J., Jeon, S., Kwon, B.O., Lee, J.H., Giesy, J.P., Khim, J.S., 2016b. Are styrene oligomers in coastal sediments of an industrial area aryl hydrocarbon-receptor agonists? Environ. Pollut. 213, 913–921. https://doi.org/10.1016/j.envpol.2016.03.025.

Horii, Y., Ohura, T., Yamashita, N., Kannan, K., 2009a. Chlorinated polycyclic aromatic hydrocarbons in sediments from industrial areas in Japan and the United States. Arch. Environ. Contam. Toxicol. 57, 651–660. https://doi.org/10.1007/s00244-009-9372-1.

Horii, Y., Khim, J.S., Higley, E.B., Giesy, J.P., Ohura, T., Kannan, K., 2009b. Relative potencies of individual chlorinated and brominated polycyclic aromatic hydrocarbons for induction of aryl hydrocarbon receptor-mediated responses. Environ. Sci. Technol. 43 (6), 2159–2165. https://doi.org/10.1021/es8030402.

Ibáñez, M., Sancho, J.V., Hernández, F., McMillan, D., Rao, R., 2008. Rapid non-target screening of organic pollutants in water by ultraperformance liquid chromatography coupled to time-of-flight mass spectrometry. Trac-Trend. Anal. Chem. 27, 481–489. https://doi.org/10.1016/j.trac.2008.03.007.

Kim, S., Lee, S., Kim, C., Liu, X., Seo, J., Jung, H., Ji, K., Hong, S., Park, J., Khim, J.S., Yoon, S., Lee, W., Park, J., Choi, K., 2014. In vitro and in vivo toxicities of sediment and surface water in an area near a major steel industry of Korea: endocrine disruption, reproduction, or survival effects combined with instrumental analysis. Sci. Total Environ. 470–471, 1509–1516. https://doi.org/10.1016/j.scitotenv.2013.08.010.

Kim, J., Hong, S., Cha, J., Lee, J., Kim, T., Lee, S., Moon, H.B., Shin, K.H., Hur, J., Lee, J.S., Giesy, J.P., Khim, J.S., 2019. Newly identified ahr-active compounds in the sediments of an industrial area using effect-directed analysis. Environ. Sci. Technol. 53, 10043–10052. https://doi.org/10.1021/acs.est.9b02166.

Kinani, S., Bouchonnet, S., Creusot, N., Bourcier, S., Balaguer, P., Porcher, J.-M., Aït-Aïssa, S., 2010. Bioanalytical characterisation of multiple endocrine- and dioxin-like activities in sediments from reference and impacted small rivers. Environ. Pollut. 158, 74–83. https://doi.org/10.1016/j.envpol.2009.07.041.

Koh, C.H., Khim, J.S., Kannan, K., Villeneuve, D.L., Senthilkumar, K., Giesy, J.P., 2004. Polychlorinated dibenzo-p-dioxins (PCDDs), dibenzofurans (PCDFs), biphenyls (PCBs), and polycyclic aromatic hydrocarbons (PAHs) and 2,3,7,8-TCDD equivalents (TEQs) in sediment from the Hyeongsan River, Korea. Environ. Pollut. 132, 489–501. https://doi.org/10.1016/j.envpol.2004.05.001.

Koh, C.H., Khim, J.S., Villeneuve, D.L., Kannan, K., Giesy, J.P., 2006. Characterization of trace organic contaminants in marine sediment from Yeongil Bay, Korea: 1. Instrumental analyses. Environ. Pollut. 142, 39–47. https://doi.org/10.1016/j.envpol.2005.09.005.

Kong, S., Lu, B., Ji, Y., Bai, Z., Xu, Y., Liu, Y., Jiang, H., 2012. Distribution and sources of polycyclic aromatic hydrocarbons in size-differentiated re-suspended dust on building surfaces in an oilfield city, China. Atmos. Environ. 55, 7–16. https://doi.org/10.1016/j.atmosenv.2012.03.044.

Larsson, M., Orbe, D., Engwall, M., 2012. Exposure time-dependent effects on the relative potencies and additivity of PAHs in the ah receptor-based H4IIE-luc bioassay. Environ. Toxicol. Chem. 31, 1149–1157. https://doi.org/10.1002/etc.1776.

Larsson, M., Giesy, J.P., Engwall, M., 2014. AhR-mediated activities of polycyclic aromatic compound (PAC) mixtures are predictable by the concept of concentration addition. Environ. Int. 73, 94–103. https://doi.org/10.1016/j.envint.2014.06.011.

Lee, S., Hong, S., Liu, X., Kim, C., Jung, D., Yim, U.H., Shim, W.J., Khim, J.S., Giesy, J.P., Choi, K., 2017a. Endocrine disrupting potential of PAHs and their alkylated analogues associated with oil spills. Environ. Sci-Proc. Imp. 19, 1117–1125. https://doi.org/10.1039/C7EM00125H.

Lee, J., Hong, S., Yoon, S.J., Kwon, B.O., Ryu, J., Giesy, J.P., Allam, A.A., Al-Khedhairy, A.A., Khim, J.S., 2017b. Long-term changes in distributions of dioxin-like and estrogenic compounds in sediments of Lake Sihwa, Korea: revisited mass balance. Chemosphere 181, 767–777. https://doi.org/10.1016/j.chemosphere.2017.04.074.

Lee, J., Hong, S., Kim, T., Lee, C., An, S.A., Kwon, B.O., Lee, S., Moon, H.B., Giesy, J.P., Khim, J.S., 2020. Multiple bioassays and targeted and nontargeted analyses to characterize potential toxicological effects associated with sediments of Masan Bay: focusing on AhR-mediated potency. Environ. Sci. Technol. 54, 4443–4454. https://doi.org/10.1021/acs.est.9b07390.

Long, E.R., Macdonald, D.D., Smith, S.L., Calder, F.D., 1995. Incidence of adverse biological effects within ranges of chemical concentrations in marine and estuarine sediments. Environ. Manag. 19, 81–97. https://doi.org/10.1007/BF02472006.

Louiz, I., Kinani, S., Gouze, M.E., Ben-Attia, M., Menif, D., Bouchonnet, S., Porcher, J.M., Ben-Hassine, O.K., Aït-Aïssa, S., 2008. Monitoring of dioxin-like, estrogenic and anti-androgenic activities in sediments of the Bizerta lagoon (Tunisia) by means of in vitro cell-based bioassays: contribution of low concentrations of polynuclear aromatic hydrocarbons (PAHs). Sci. Total Environ. 402, 318–329. https://doi.org/10.1016/j.scitotenv.2008.05.005.

Macdonald, D.D., Carr, R.S., Calder, F.D., Long, E.R., Ingersoll, C.G., 1996. Development and evaluation of sediment quality guidelines for Florida coastal waters. Ecotoxicology 5, 253–278. https://doi.org/10.1007/BF00118995.

Marzo, M., Kulkarni, S., Manganaro, A., Roncaglioni, A., Wu, S., Barton-Maclaren, T.S., Lester, C., Benfenati, E., 2016. Integrating in silico models to enhance predictivity for developmental toxicity. Toxicology 370, 127–137. https://doi.org/10.1016/j.tox.2016.09.015.

Mekenyan, O.G., Veith, G.D., Call, D.J., Ankley, G.T., 1996. A qsar evaluation of ah receptor binding of halogenated aromatic xenobiotics. Environ. Health Perspect. 104, 1302–1310. https://doi.org/10.1289/ehp.961041302.

Mitchell, K.A., Elferink, C.J., 2009. Timing is everything: consequences of transient and sustained AhR activity. BBA-Gen. Subjects 77, 947–956. https://doi.org/10.1016/j.bcp.2008.10.028.

Moschet, C., Anumol, T., Lew, B.M., Bennett, D.H., Young, T.M., 2018. Household dust as a repository of chemical accumulation: new insights from a comprehensive high-resolution mass spectrometric study. Environ. Sci. Technol. 52, 2878–2887. https://doi.org/10.1021/acs.est.7b05767.

Muz, M., Krauss, M., Kutsarova, S., Schulze, T., Brack, W., 2017. Mutagenicity in surface waters: synergistic effects of carboline alkaloids and aromatic amines. Environ. Sci. Technol. 51, 1830–1839. https://doi.org/10.1021/acs.est.6b05468.

Ouyang, X., Weiss, J.M., de Boer, J., Lamoree, M.H., Leonards, P.E.G., 2017. Non-target analysis of household dust and laundry dryer lint using comprehensive two-dimensional liquid chromatography coupled with time-of-flight mass spectrometry. Chemosphere 166, 431–437. https://doi.org/10.1016/j.chemosphere.2016.09.107.

Pizzo, F., Lombardo, A., Manganaro, A., Benfenati, E., 2013. In silico models for predicting ready biodegradability under REACH: a comparative study. Sci. Total Environ. 463–464, 161–168. https://doi.org/10.1016/j.scitotenv.2013.05.060.

Ravindra, K., Wauters, E., Van Grieken, R., 2008. Variation in particulate PAHs levels and their relation with the transboundary movement of the air masses. Sci. Total Environ. 396, 100–110. https://doi.org/10.1016/j.scitotenv.2008.02.018.

Schymanski, E.L., Singer, H.P., Slobodnik, J., Ipolyi, I.M., Oswald, P., Krauss, M., Schulze, T., Haglund, P., Letzel, T., Grosse, S., Thomaidis, N.S., Bletsou, A., Zwiener, C., Ibáñez, M., Portolés, T., de Boer, R., Reid, M.J., Onghena, M., Kunkel, U., Schulz, W., Guillon, A., Noyon, N., Leroy, G., Bados, P., Bogialli, S., Stipanicev, D., Rostkowski, P., Hollender, J., 2015. Non-target screening with high-resolution mass spectrometry: critical review using a collaborative trial on water analysis. Anal. Bioanal. Chem. 407, 6237–6255. https://doi.org/10.1007/s00216-015-8681-7.

Shipley, J.M., Waxman, D.J., 2006. Aryl hydrocarbon receptor-independent activation of estrogen receptor-dependent transcription by 3-methycholanthrene. Toxicol. Appl. Pharm. 213, 87–97. https://doi.org/10.1016/j.taap.2005.09.011.

Simon, E., van Velzen, M., Brandsma, S.H., Lie, E., Løken, K., de Boer, J., Bytingsvik, J., Jenssen, B.M., Aars, J., Hamers, T., Lamoree, M.H., 2013. Effect-directed analysis to explore the polar bear exposome: identification of thyroid hormone disrupting compounds in plasma. Environ. Sci. Technol. 47, 8902–8912. https://doi.org/10.1021/es401696u.

Takahashi, T., Takenobu, T., Takeya, J., Iwasa, Y., 2007. Ambipolar light-emitting transistors of a tetracene single crystal. Adv. Funct. Mater. 17, 1623–1628. https://doi.org/10.1002/adfm.200700046.

Vedani, A., Dobler, M., Hu, Z., Smieško, M., 2015. OpenVirtualToxLab-a platform for generating and exchanging in silico toxicity data. Toxicol. Lett. 232, 519–532. https://doi.org/10.1016/j.toxlet.2014.09.004.

Venkataraman, C., Lyons, J.M., Friedlander, S.K., 1994. Size distributions of polycyclic aromatic hydrocarbons and elemental carbon. 1. Sampling, measurement methods, and source characterization. Environ. Sci. Technol. 28, 555–562. https://doi.org/10.1021/es00053a005.

Villeneuve, D.L., Kannan, K., Khim, J.S., Falandysz, J., Nikiforov, V.A., Blankenship, A.L., Giesy, J.P., 2000. Relative potencies of individual polychlorinated naphthalenes to induce dioxin-like responses in fish and mammalian in vitro bioassays. Arch. Environ. Contam. Toxicol. 39, 273–281. https://doi.org/10.1007/s002440010105.

Yang, B., Zhou, L., Xue, N., Li, F., Li, Y., Vogt, R.D., Cong, X., Yan, Y., Liu, B., 2013. Source apportionment of polycyclic aromatic hydrocarbons in soils of huanghuai plain, China: comparison of three receptor models. Sci. Total Environ. 443, 31–39. https://doi.org/10.1016/j.scitotenv.2012.10.094.

Yu, S., Campiglia, A.D., 2005. Direct determination of dibenzo[a, l]pyrene and its four dibenzopyrene isomers in water samples by solid-liquid extraction and laser-excited time-resolved Shpol'skii spectrometry. Anal. Chem. 77, 1440–1447. https://doi.org/10.1021/ac048310d.

Zedda, M., Zwiener, C., 2012. Is nontarget screening of emerging contaminants by LC-HRMS successful? A plea for compound libraries and computer tools. Anal. Bioanal. Chem. 403, 2493–2502. https://doi.org/10.1007/s00216-012-5893-y.

Zhang, Y., Guo, C.-S., Xu, J., Tian, Y.-Z., Shi, G.-L., Feng, Y.-C., 2012. Potential source contributions and risk assessment of PAHs in sediments from Taihu Lake, China: comparison of three receptor models. Water Res. 46, 3065–3073. https://doi.org/10.1016/j.watres.2012.03.006.

Zhang, J., You, J., Li, H., Mehler, W.T., Zeng, E.Y., 2018. Particle-scale understanding of cypermethrin in sediment: desorption, bioavailability, and bioaccumulation in benthic invertebrate Lumbriculus variegatus. Sci. Total Environ. 642, 638–645. https://doi.org/10.1016/j.scitotenv.2018.06.098.

Zhang, J., Li, R., Zhang, X., Bai, Y., Cao, P., Hua, P., 2019. Vehicular contribution of PAHs in size dependent road dust: a source apportionment by PCA-MLR, PMF, and unmix receptor models. Sci. Total Environ. 649, 1314–1322. https://doi.org/10.1016/j.scitotenv.2018.08.410.

Zwart, N., Jonker, W., Broek, R.T., de Boer, J., Somsen, G., Kool, J., Hamers, T., Houtman, C.J., Lamoree, M.H., 2020. Identification of mutagenic and endocrine disrupting compounds in surface water and wastewater treatment plant effluents using high-resolution effect-directed analysis. Water Res. 168, 115204. https://doi.org/10.1016/j.watres.2019.115204.

<Supplementary Materials>

Effect-directed identification of novel aryl hydrocarbon receptor-active aromatic compounds in coastal sediments collected from a highly industrialized area

Jiyun Gwak [1], Jihyun Cha [1], Junghyun Lee, Youngnam Kim, Seong-Ah An, Sunggyu Lee, Hyo-Bang Moon, Jin Hur, John P. Giesy, Seongjin Hong*, Jong Seong Khim*

This PDF file includes:

Number of pages: 17

Number of Supplementary Tables: 11, Tables S1 to S11

Number of Supplementary Figures: 2, Figs. S1 to S2

References

[1] These authors contributed equally to this work.

***Corresponding authors.**

E-mail addresses: hongseongjin@cnu.ac.kr (S. Hong); jskocean@snu.ac.kr (J.S. Khim).

Supplementary Tables

Table S1. Reverse phase(RP)-HPLC conditions for fractionation of silica gel column fractions (Hong et al., 2016).

Instrument	Agilent 1260 HPLC system (Preparative scale) 1260 Multiple wavelength detector
Column	PrepHT XDB-C18 reverse phase column (250 mm × 21.2 mm × 7 μm)
Mobile phase	A: Water, B: Methanol
Flow rate	10 mL min^{-1}
Injection volume	1 mL
Mobile phase gradient	40% A (0 min) → 40–0% A (0–40 min) → 0% A (40–60 min) → 0–40% A (60–62 min) → 40% A (62–70 min) 60% B (0 min) → 60–100% B (0–40 min) → 100% B (40–60 min) → 100–60% B (60–62 min) → 60% B (62–70 min)
Test standards	34 polychlorinated biphenyls 16 polycyclic aromatic hydrocarbons 7 alkylphenols 5 phthalates
Fractions collected times	

RP-HPLC Sub-fraction	Starting –End sampling time (min.)	Volume (mL)	Log Kow
1	3.11 – 6.35	38	< 1
2	6.35 – 12.83	65	1 – 2
3	12.83 – 19.32	65	2 – 3
4	19.32 – 25.80	65	3 – 4
5	25.80 – 32.29	65	4 – 5
6	32.29 – 38.78	65	5 – 6
7	38.78 – 45.26	65	6 – 7
8	45.26 – 51.70	65	7 – 8
9	51.70 – 58.23	65	8 – 9
10	58.23 – 64.72	65	> 9

Table S2. Description of the experimental design for H4IIE-*luc in vitro* bioassay.

Bioassay		**In vitro assays**
		H4IIE-*luc*
Endpoint		AhR-mediated potencies
Test samples		Raw extracts, silica gel fractions, RP-HPLC fractions
Experimental conditions	**Test chamber**	96-well plate
	Solvent carrier	0.1% DMSO
	Temperature (°C)	37
	Test duration	4 h
	Initial concentrations	7.0×10^4 cells mL^{-1}
Replicates		3
Positive control		Benzo[*a*]pyrene

Table S3. Instrumental conditions of GC-MSD for PAHs and SOs analyses.

Instrument	GC: Agilent Technologies 7890B MSD: Agilent Technologies 5977A
Column	DB-5MS (30 m × 0.25 mm i.d. × 0.25 μm film)
Carrier gas	He
Flow rate	1.0 mL $min.^{-1}$
Injection volume	1 μL
Mass range	50−600 *m*/*z*
Ion source temperature	230 °C
Ionization mode	EI mode (70 eV)
Oven temperature	60 °C (hold 2 min) → 6 °C min^{-1} to 300 °C (hold 13 min)

Table S4. Target compounds, abbreviations, target ions, and method detection limit in the instrumental analysis and method detection limits and recoveries of surrogate standards.

Target compounds	Abbreviation	Target ions		Method detection limit ($ng\ g^{-1}$ dm)
		Quantification ion	Confirmation ion	
Traditional PAHs (t-PAHs)				
Acenaphthene	Ace	153	154, 152	3.1
Acenaphthylene	Acl	152	151, 150	3.7
Fluorene	Flu	166	165, 167	3.1
Phenanthrene	Phe	178	176, 179	3.1
Anthracene	Ant	178	176, 179	3.9
Fluoranthene	Fl	202	200, 101	4.1
Pyrene	Py	202	200, 101	4.7
Benzo[*a*]anthracene	BaA	228	226, 229	12
Chrysene	Chr	228	226, 229	3.0
Benzo[*b*]fluoranthene	BbF	252	253, 250	2.6
Benzo[*k*]fluoranthene	BkF	252	253, 251	3.2
Benzo[*a*]pyrene	BaP	252	253, 126	1.1
Indeno[*1,2,3-cd*]pyrene	IcdP	276	138, 137	3.0
Dibenz[*a,h*]anthracene	DbahA	278	276, 279	2.2
Benzo[*g,h,i*]perylene	BghiP	276	138, 137	3.8
Emerging PAHs (e-PAHs)				
3-Methylphenanthrene	3MP	192	191, 189	0.06
2-Methylphenanthrene	2MP	192	191, 189	0.17
2-Methylanthracene	2MA	192	191, 189	2.6
9-Ethylphenanthrene	9EP	191	206, 189	6.8
1,6-Dimethylphenanthrene	16DMP	206	191, 189	0.23
1,2-Dimethylphenanthrene	12DMP	206	191, 189	0.21
Benzo[*b*]naphtho[*2,3-d*]furan	BBNF	218	189, 219	1.4
11H-Benzo[*b*]fluorene	11BbF	216	215, 213	4.0
Benzo[*b*]naphtho[*2,1*-d]thiophene	BBNT	234	235, 232	3.4
Triphenylene	Trl	228	226, 229	0.21
3-Methylchrysene	3MC	242	241, 239	0.26
5-Methylbenz[*a*]anthracene	5MBA	256	241, 239	2.8
1,12-dimethylbenzo[*c*]phenanthrene	BCP	242	241, 239	5.2
1-Methylchrysene	1MC	242	241, 293	0.14
Benzo[*j*]fluoranthene	BjF	252	253, 250	2.1
Benzo[*e*]pyrene	BEP	252	250, 253	3.7
11H-benzo[*a*]fluorene	11BaF	216	215, 216	0.34
4,5-Methanochrysene	4,5MC	239	240, 241	1.6
Benz[*b*]anthracene	BbA	228	226, 229	0.32
Styrene oligomers (SOs)				
1,3-Diphenylpropane	SD1	92	196, 105	0.19
cis-1,2-Diphenylcyclobutane	SD2	104	208, 78	0.18
2,4-Diphenyl-1-butene	SD3	91	208, 104	0.89
trans-1,2-Diphenylcyclobutane	SD4	104	208, 78	0.11
2,4,6-Triphenyl-1-hexene	ST1	91	117, 194	0.63
1e-Phenyl-4e-(1-phenylethyl)-tetralin	ST2	91	129, 207	0.66
1a-Phenyl-4e-(1-phenylethyl)-tetralin	ST3	91	129, 207	0.31
1a-Phenyl-4a-(1-phenylethyl)-tetralin	ST4	91	129, 207	0.70
1e-Phenyl-4a-(1-phenylethyl)-tetralin	ST5	91	129, 207	0.41
1,3,5-Triphenylcyclohexane	ST6	117	104, 130	0.88
Internal standard				
2-Fluorobiphenyl	IS	172	171, 170	

Table S5. Instrumental conditions of GC-QTOFMS for full-scan screening analysis.

Instrument	GC: Agilent Technologies 7890B QTOFMS: Agilent Technologies 7200
Samples	S1 (F2.6, F2.7, and F2.8)
Column	DB-5MS UI (30 m × 0.25 mm i.d. × 0.25 μm film)
Carrier gas	He
Flow rate	1.2 mL $min.^{-1}$
Injection volume	2 μL
Mass range	50–800 *m*/*z*
Ion source temperature	230 °C
Ionization mode	EI mode (70 eV)
Software	Qualitative analysis B.07.01 MassHunter Quantitative analysis Unknown analysis NIST Library (ver. 2014)

Table S6. Molecular formula, GC/MS retention time, fragment ions, and relative potency values for AhR-active compounds reported previously.

Compounds	Abb.[a]	Molecular formula	Molecular weight	GC RT[b] (min.)	Mass fragment ions (*m*/*z*)	ReP values	References
Traditional PAHs							
Benz[*a*]anthracene	BaA	$C_{18}H_{12}$	228	33.87	*228*[c], 226, 229[d]	3.2×10^{-1}	Kim et al. (2019)
Chrysene	Chr	$C_{18}H_{12}$	228	34.01	*228*, 226, 229	8.5×10^{-1}	
Benzo[*b*]fluoranthene	BbF	$C_{20}H_{12}$	252	37.85	*252*, 253, 250	5.0×10^{-1}	
Benzo[*k*]fluoranthene	BkF	$C_{20}H_{12}$	252	37.94	*252*, 253, 251	4.8×10^{-1}	
Benzo[*a*]pyrene	BaP	$C_{20}H_{12}$	252	38.90	*252*, 253, 126	1.0	
Indeno[*1,2,3-c,d*]pyrene	IcdP	$C_{22}H_{12}$	276	42.33	*276*, 138, 137	5.8×10^{-1}	
Dibenz[*a,h*]anthracene	DbahA	$C_{22}H_{14}$	278	42.47	*278*, 276, 279	6.6×10^{-1}	
Emerging PAHs							
Benzo[*b*]naphtho[*2,3-d*]furan	BBNF	$C_{16}H_{10}O$	218	29.88	*218*, 189, 219	8.2×10^{-2}	Kim et al. (2019)
11H-Benzo[*b*]fluorene	11BbF	$C_{17}H_{12}$	216	30.99	*216*, 215, 213	2.4×10^{-1}	
Benzo[*b*]naphtho[*2,1-d*]thiophene	BBNT	$C_{16}H_{10}S$	234	33.09	*234*, 235, 232	3.6×10^{-2}	
3-Methylchrysene	3MC	$C_{19}H_{14}$	242	35.71	*242*, 241, 239	1.5	
5-Methylbenz[*a*]anthracene	5MBA	$C_{19}H_{14}$	242	35.99	*242*, 241, 239	4.2×10^{-1}	
1-Methylchrysene	1MC	$C_{19}H_{14}$	242	36.18	*242*, 241, 239	6.0	
Benzo[*j*]fluoranthene	BjF	$C_{20}H_{12}$	252	38.03	*252*, 253, 250	1.7	
11H-Benzo[*a*]fluorene	11BaF	$C_{17}H_{12}$	216	30.20	*216*, 215, 213	1.2	Cha et al. (2019)
Benz[*b*]anthracene	BbA	$C_{18}H_{12}$	228	34.56	*228*, 226, 229	10.6	
4,5-Methanochrysene	4,5MC	$C_{19}H_{12}$	234	35.76	*240*, 239, 241	1.0	
Styrene Oligomers							
1,3-Diphenylpropane	SD1	$C_{15}H_{16}$	196	21.10	*92*, 196, 105	2.3×10^{-3}	Hong et al. (2016)
2,4-Diphenyl-1-butene	SD3	$C_{16}H_{16}$	208	22.35	*91*, 208, 104	3.0×10^{-4}	
1e-Phenyl-4e-(1-phenylethyl)-tetralin	ST2	$C_{24}H_{24}$	312	33.52	*91*, 117, 194, 207	2.7×10^{-3}	

[a] Abb.: Abbreviations.
[b] GC RT: Gas chromatography retention time.
[c] Quantification ion.
[d] Confirmation ions.

Table S7. Concentrations of PAHs and SOs in the sediments of Yeongil Bay, South Korea.

Chemical class	Compounds	Abb.[a]	Organic extracts of sediments (ng g^{-1} dry mass)					
			S1	S2	S3	S4	S5	S6
PAHs	Acenaphthene	Ace	6100	< LOD[b]	< LOD	< LOD	< LOD	< LOD
	Acenaphthylene	Acl	1200	< LOD	< LOD	< LOD	3.1	< LOD
	Fluorene	Flu	19000	2.2	< LOD	< LOD	< LOD	< LOD
	Phenanthrene	Phe	56000	22	3.4	4.2	15	< LOD
	Antracene	Ant	11000	13	< LOD	< LOD	< LOD	< LOD
	Fluoranthene	Fl	42000	< LOD	4.5	6.8	20	< LOD
	Pyrene	Py	24000	67	5.4	6.2	20	< LOD
	Benzo[*a*]anthracene	BaA	13000	24	< LOD	< LOD	< LOD	< LOD
	Chrysene	Chr	12000	22	0.73	1.8	8.8	< LOD
	Benzo[*b*]fluoranthene	BbF	19000	25	< LOD	< LOD	4.3	< LOD
	Benzo[*k*]fluoranthene	BkF	2300	5.1	< LOD	< LOD	< LOD	< LOD
	Benzo[*a*]pyrene	BaP	7000	9.1	3.3	1.6	8.1	< LOD
	Indeno[*1,2,3-cd*]pyrene	IcdP	1400	4.1	< LOD	< LOD	4.8	< LOD
	Dibenz[*a,h*]anthracene	DbahA	2200	< LOD	< LOD	< LOD	< LOD	< LOD
	Benzo[*g,h,i*]perylene	BghiP	4800	5.6	< LOD	< LOD	7.3	< LOD
	3-Methylphenanthrene	3MP	3300	4.3	0.4	0.8	2.6	0.6
	2-Methylphenanthrene	2MP	9200	2.3	1.6	3.5	11	2.4
	2-Methylanthracene	2MA	3400	4.6	1.0	1.1	3.5	0.7
	9-Ethylphenanthrene	9EP	180	<LOD	<LOD	<LOD	0.7	<LOD
	1,6-Dimethylphenanthrene	16DMP	5300	0.3	2.3	0.4	9.1	0.3
	1,2-Dimethylphenanthrene	12DMP	23	<LOD	<LOD	<LOD	0.1	<LOD
	Benzo[*b*]naphtho[*2,3-d*]furan	BBNF	3200	6.2	<LOD	0.2	<LOD	<LOD
	11H-Benzo[*b*]fluorene	11BbF	2700	3.1	0.8	1.3	3.1	0.1
	Benzo[*b*]naphtho[*2,1*-d]thiophene	BBNT	3000	0.1	<LOD	<LOD	<LOD	<LOD
	Triphenylene	TRI	1900	67	2.3	1.3	12	2.4
	3-Methylchrysene	3MC	1100	<LOD	<LOD	<LOD	<LOD	<LOD
	5-Methylbenz[*a*]anthracene	5MBA	220	<LOD	<LOD	<LOD	<LOD	<LOD
	1,12-dimethylbenzo[*c*]phenanthrene	BCP	1100	0.4	<LOD	0.3	<LOD	<LOD
	1-Methylchrysene	1MC	21	<LOD	<LOD	<LOD	<LOD	<LOD
	Benzo[*j*]fluoranthene	BjF	12000	14	6.8	3.1	9.7	1.7
	Benzo[*e*]pyrene	BEP	10000	17	0.6	3.2	5.8	4.2
	11H-benzo[a]fluorene	11BaF	9600	30	1.5	2.4	5.3	1.2
	4,5-Methanochrysene	4,5MC	2400	3.0	0.0	0.0	3.2	0.0
	Benz[*b*]anthracene	BbA	1100	29	0.4	0.0	0.8	0.0
Styrene Oligomers	1,3-Diphenylproane	SD1	6.3	1.6	<LOD	< LOD	< LOD	1.7
	cis-1,2-Diphenylcyclobutane	SD2	<LOD	< LOD	< LOD	<LOD	< LOD	< LOD

	2,4-Diphenyl-1-butene	SD3	98	56	52	26	36	66
	trans-1,2-Diphenylcyclobutane	SD4	<LOD	< LOD	< LOD	<LOD	< LOD	< LOD
	4,6-Triphenyl-1-hexene	ST1	16	12	12	12	18	12
	1e-Phenyl-4e-(1-phenylethyl)-tetralin	ST2	<LOD	< LOD	< LOD	<LOD	< LOD	< LOD
	1a-Phenyl-4e-(1-phenylethyl)-tetralin	ST3	<LOD	< LOD	< LOD	<LOD	< LOD	< LOD
	1a-Phenyl-4a-(1-phenylethyl)-tetralin	ST4	<LOD	< LOD	< LOD	<LOD	< LOD	< LOD
	1e-Phenyl-4a-(1-phenylethyl)-tetralin	ST5	<LOD	< LOD	< LOD	<LOD	< LOD	< LOD
	1,3,5-Triphenylcyclohexane (isomer mix)	ST6	25	<LOD	< LOD	< LOD	<LOD	< LOD

[a] Abb.: Abbreviations.

[b] < LOD: Below detection limits.

Table S8. List of candidates for AhR-active compounds in the fraction samples (F2.6, F2.7, and F2.8) of organic extracts from S1 sediment using GC-QTOFMS. AhR binding potencies of compounds were measured using H4IIE-*luc* bioassays and VirtualToxLab modeling.

Fractions and compounds	Molecular formula	CAS number	Molecular weight	Library Matching factor	AhR binding affinity H4IIE-*luc* bioassay	AhR binding affinity VirtualToxLab modeling [a]
F2.6 fraction						
4,5-Dihydropyrene	$C_{16}H_{12}$	6628-98-4	204.266	97		5.60 µm
Benzo[*ghi*]fluoranthene	$C_{18}H_{10}$	203-12-3	226.272	97		1.69 µm
4,5,9,10-Tetrahydropyrene	$C_{16}H_{14}$	781-17-9	206.282	92		3.92 µm
Benzo[*c*]phenanthrene	$C_{18}H_{12}$	195-19-7	228.288	90		890 nm
5(*12h*)-Naphthacenone	$C_{18}H_{12}O$	3073-99-2	244.287	87		69.3 nm
4H-Naphtho[*1,2,3,4-def*]carbazole	$C_{18}H_{11}N$	109606-75-9	167.207	85		3.18 µm
Pyreno[*2,1-b*]furan	$C_{18}H_{10}O$	96918-24-0	242.271	83		646 nm
7,12-Dihydrobenz[*a*]anthracene	$C_{18}H_{14}$	16434-59-6	230.304	83		309 nm
Dibenzo[*b,def*]carbazole	$C_{18}H_{11}N$	104313-09-9	241.287	82		n.a [b]
1-Aminopyrene	$C_{16}H_{11}N$	1606-67-3	217.265	76		4.21 µm
F2.7 fraction						
Benzo[*b*]triphenylene	$C_{22}H_{14}$	215-58-7	278.347	95		104 nm
2,2'-Binaphthalene	$C_{20}H_{14}$	612-78-2	254.325	95		57.0 nm
Picene	$C_{22}H_{14}$	213-46-7	278.347	93		95.5 nm
4,5-Dihydrobenzo[*def*]chrysene	$C_{20}H_{14}$	57652-66-1	254.325	93		392 nm
10-Methylbenzo[*a*]pyrene	$C_{21}H_{14}$	63104-32-5	266.336	92	+[c]	521 nm
2-Methylpyrene	$C_{17}H_{12}$	3442-78-2	216.277	91		2.83 µm
1-Phenylpyrene	$C_{22}H_{14}$	5101-27-9	278.347	91		48.4 nm
1,1'-Binaphthalene	$C_{20}H_{14}$	604-53-5	254.325	90		292 nm
7,8-Dihydrobenzo[*a*]pyrene	$C_{20}H_{14}$	17573-23-8	254.325	90		351 nm
2-Methylbenzo[*c*]phenanthrene	$C_{19}H_{14}$	2606-85-1	242.314	88		676 nm
1,9-Dihydropyrene	$C_{16}H_{12}$	28862-02-4	204.266	86		5.03 µm
2,2'-Bis(*quinoline*)	$C_{18}H_{12}N_2$	119-91-5	256.301	85		–
1,2,3,6b,7,8-Hexahydrobenzo[*j*]fluoranthene	$C_{20}H_{18}$	18522-48-0	258.357	83		n.a
1-(2-naphthalenylmethyl)Naphthalene	$C_{21}H_{16}$	611-48-3	268.352	83		32.7 nm
1,2'-Binaphthalene	$C_{20}H_{14}$	4325-74-0	254.325	82		111 nm
9H-Cyclopenta[*a*]pyrene	$C_{19}H_{12}$	50861-05-7	240.299	82		976 nm
1,1'-bis-Acenaphthylidene	$C_{24}H_{16}$	2435-82-7	304.384	81		51.6 nm
Dinaphtho[*1,2-b:2',1'-d*]thiophene	$C_{20}H_{12}S$	239-72-5	284.374	80		163 nm
11H-Indeno[*2,1-a*]phenanthrene	$C_{21}H_{14}$	220-97-3	266.336	79		112 nm
1,2-Diphenylacenaphthylene	$C_{24}H_{16}$	2000543-62-9	304.384	79		20.5 nm
2-Hydroxy-9-phenyl-1H-Phenalen-1-one	$C_{19}H_{12}O_2$	56252-32-5	272.297	78		51.7 nm

7,12-Dimethylbenz[*a*]anthracene	$C_{20}H_{16}$	57-97-6	256.341	77	+	654 nm
1-Methyl-7-(1-methylethyl)phenanthrene	$C_{18}H_{18}$	483-65-8	234.335	77		405 nm
9-Phenylanthracene	$C_{20}H_{14}$	602-55-1	254.325	76		245 nm
1,9-Dimethylpyrene	$C_{18}H_{14}$	74298-70-7	230.304	76		2.63 µm
3-(5-Methylpyridin-2-yl)quinoline	$C_{15}H_{12}N_2$	2000265-01-4	220.269	74		190 nm
8H-Indeno[*2,1-b*]phenanthrene	$C_{21}H_{14}$	241-28-1	266.336	74		88.2 nm
4-(2-Methylimidazo[*1,2-a*]pyridin-3-yl)-N-(4-trifluoro methyl)-phenyl)-pyrimidin-2-amine	$C_{19}H_{14}F_3N_5$	2000721-71-9	369.343	74		–
2,4-bis(1-phenylethyl)-Phenol	$C_{22}H_{22}O$	2769-94-0	302.409	74		43.7 nm
13H-Dibenzo[*a,h*]fluorene	$C_{21}H_{14}$	239-85-0	266.336	73		n.a
2-Hydroxy-7H-benzo[*c*]fluoren-7-one	$C_{17}H_{10}O_2$	2000351-07-0	246.260	73		n.a
Naphtho[*2,1,8,7-klmn*]xanthene	$C_{18}H_{10}O$	191-37-7	242.271	73		1.47 µm
8,12-Dimethylbenz(*a*)anthracene	$C_{20}H_{16}$	20627-31-0	256.341	71		426 nm
4-Benzylbiphenyl	$C_{19}H_{16}$	613-42-3	244.330	71		n.a
1-Methyl-4-p-tolylnaphthalene	$C_{18}H_{16}$	93870-57-6	232.320	70		479 nm
7-Methylbenz[*a*]anthracene	$C_{19}H_{14}$	2541-69-7	242.314	88	+	461 nm
F2.8 fraction						
1,2:4,5-Dibenzopyrene	$C_{24}H_{14}$	192-65-4	302.368	89		58.5 nm
6,6'-Biquinoline	$C_{18}H_{12}N_2$	612-79-3	256.301	84		27.9 nm
2-Pyrenol	$C_{16}H_{10}O$	78751-58-3	218.250	84		4.21 µm
Dibenzo[*e,l*]pyrene	$C_{24}H_{14}$	192-51-8	302.368	82	–[d]	201 nm
7,12-Dihydro-2-methylbenz[*a*]anthracene	$C_{19}H_{16}$	35187-44-1	244.330	81		311 nm
20-Methylcholanthrene	$C_{21}H_{16}$	56-49-5	268.352	80	+	195 nm
8-Hydroxyindeno[*1,2,3-cd*]pyrene	$C_{22}H_{12}O$	99520-58-8	292.330	77		99.6 nm
8-Phenylacenaphtho[*1,2-b*]pyridine	$C_{21}H_{13}N$	2000461-93-4	279.334	75		n.a
6,13-Dihydrodibenzo[*b,i*]phenazine	$C_{20}H_{14}N_2$	10350-06-8	288.339	74		n.a
7H-Benzimidazo[*2,1-a*]benzo[*de*]isoquinoline-7-thione	$C_{18}H_{10}N_2S$	2000484-30-3	286.350	73		38.8 nm
Anthra[*2,3-b*]benzo[*d*]thiophene	$C_{20}H_{12}S$	249-05-8	284.374	73		82.5 nm
Coronene	$C_{24}H_{12}$	191-07-1	300.352	72		–
Benzo[*b*]naphthacene	$C_{22}H_{14}$	135-48-8	278.347	72	–	n.a

[a] Green: none binding, blue: low binding, red: moderate binding, grey: elevated binding.
[b] n.a: not available.
[c] +: Significant response in the H4IIE-*luc* bioassay.
[d] –: Not significant response in the H4IIE-*luc* bioassay.

Table S9. Relative potency values for newly identified AhR agonists relative to the potency of BaP in the H4IIE-*luc* bioassay.

Compounds	Maximum concentration (nM)[a]	%BaP_{max}	Slope	Relative $potency_{20\text{-}50\text{-}80}$[b]	
				ReP_{50}	$ReP_{20\text{-}80}$
BaP	50	100	42	1.0	1.0-1.0
7,12DbA	39	67	29	0.2	0.1-0.4
20MC	37	175	78	3.2	1.5-6.9
10MbA	38	91	41	1.2	1.2-1.2
7MbA	41	105	40	1.4	1.3-1.5

[a] 0.1% dosing concentration.

[b] RePs reported as the range of ReP estimates generated from multiple points over a response range from 20 to 50 to 80 %BaP_{max}.

Table S10. Molecular formula, GC/MSD retention time, and fragment ions for novel AhR-active compounds.

Compounds	Abb.[a]	Molecular formula	Molecular weight	GC RT[b] (min.)	Mass fragment ions (*m*/*z*)
7,12-dimethylbenz[*a*]anthracene	7,12DbA	$C_{20}H_{16}$	256	38.77	*256*[c], 241, 239[d]
10-methylbenz[*a*]pyrene	10MbA	$C_{18}H_{12}$	266	41.51	*266*, 265, 263
7-methylbenz[*a*]anthracene	7MbA	$C_{19}H_{14}$	242	37.15	*242*, 241, 239
20-methylcholanthrene	20MC	$C_{21}H_{16}$	268	41.01	*268*, 252, 253

[a] Abb.: Abbreviations.
[b] GC RT: Gas chromatography retention time.
[c] Quantification ion.
[d] Confirmation ions.

Table S11. Benzo[*a*]pyrene equivalent concentrations (BEQs) and contributions to total induced AhR-mediated potencies in sediments obtained from this study and previous studies in the coastal waters of Korea.

Target compounds	AhR agonists	Sampling sites							
		Ulsan Bay (*n* = 4)		Lake Sihwa (*n* = 8)		Masan Bay (*n* = 2)		Yeongil Bay (*n* = 6)	
		BEQs (ng g^{-1} dm)	Contribution (%)	BEQs (ng g^{-1} dm)	Contribution (%)	BEQs (ng g^{-1} dm)	Contribution (%)	BEQs (ng g^{-1} dm)	Contribution (%)
Traditional PAHs	BaA	1.0–93	0.78–69	0.03–1.0	0.22–37	7–12	0.017–0.038	8.5–800	2.5–3.5
	Chr	4.0–290	1.3–220	0.30–63	0.90–18	4.5–5.1	0.012–0.015	20–1200	5.3–6.1
	BbF	2.8–180	0.3–2.7	0.10–44	0.48–2.1	11–16	0.033–0.036	12–990	0.16–0.23
	BkF	2.4–42	4.6–36	0.09–110	0.22–1.9	1.1–1.9	0.0042–0.033	2.4–317	0.51–0.87
	BaP	3.3–260	3.0–20	1.0–70	0.37–1.9	5.4–8.7	0.016–0.019	1.6–1000	0.18–0.21
	IcdP	3–122	2.0–18	0.10–30	0.01–0.29	3.4–6.3	0.0059–0.0047	2.2–370	0.26–0.39
	DbahA	0.5–49	2.5–16	0.02-63	0.05–0.11	2.1–2.4	0.0094–0.012	0.0–190	0.001–0.06
Emerging PAHs	BjF	7.7–130	4.0–22					73–20000	7.0–10
	BBNF	0.78–12	0.16–11					0.0–300	0–1.3
	BBNT	0.03–3.9	0.01–0.43					0.07–120	0.0034–0.06
	11BbF	0.4–26	1.3–12					2.8–760	0.29–0.39
	3MC	3.15–130	1.4–7.0					14–1700	0.85–1.3
	5MBA	0.3–6.3	0–1.7					3.2–93	0.04–0.3
	1MC	41–96	0–12					59–130	0.069–5.6
	4,5MC			6.0–43	0.46–2.9			4.2–3300	0.40–1.7
	BbA			1.2–210	1.1–68			300–12000	0.5–90
	11BaF			4.8–330	0.77–22			1.2–9600	3.0–5.2
Newly identified AhR agonists	10MbA							0.1–580	0.29–0.46
	7,12BaA							4.9 –79	0.007–0.04
	7MBaA							1.7–170	0.09–0.2
	20MC							2.0–200	0.59–1.7
References		Kim et al. (2019)		Cha et al. (2019)		Lee et al. (2020)		This study	

LOD: Below detection limits.

Supplementary Figures

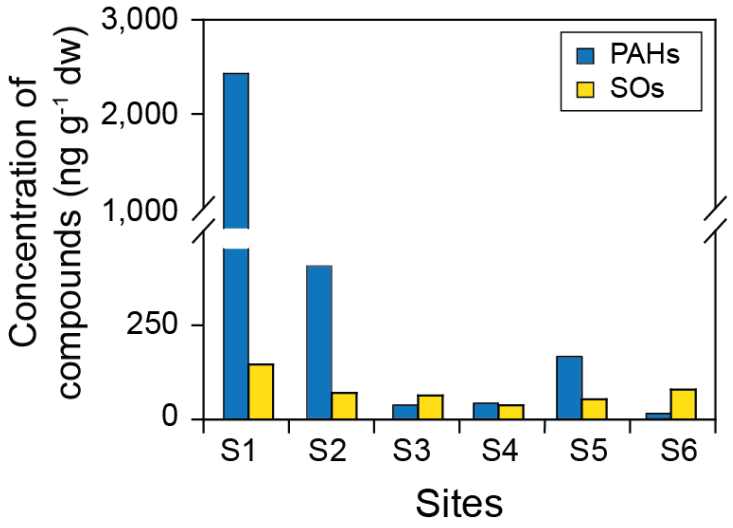

Fig. S1. Concentrations of PAHs and SOs in the sediments of Yeongil Bay, South Korea.

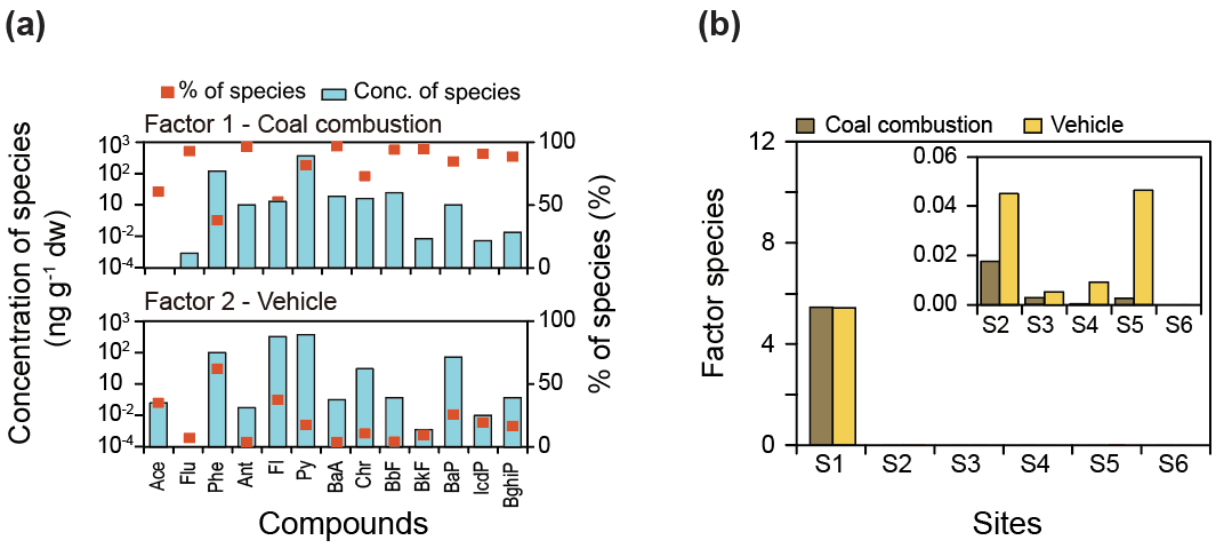

Fig. S2. Source identification and contribution of PAHs in the sediments analyzed in the present study. (a) Factor profiles and (b) factor scores generated by the PMF model.

References

Cha, J., Hong, S., Kim, J., Lee, J., Yoon, S.J., Lee, S., Moon, H.-B., Shin, K.-H., Hur, J., Giesy, J.P., Khim, J.S., 2019. Major AhR-active chemicals in sediments of Lake Sihwa, South Korea: Application of effect-directed analysis combined with full-scan screening analysis. Environ. Int. 133, 105199.

Hong, S., Lee, J., Lee, C., Yoon, S. J., Jeon, S., Kwon, B.O., Lee, J.H., Giesy, J.P., Khim, J.S., 2016. Are styrene oligomers in coastal sediments of an industrial area aryl hydrocarbon-receptor agonists? Environ. Pollut. 213, 913-921.

Kim, J., Hong, S., Cha, J., Lee, J., Kim, T., Lee, S., Moon, H.-B., Shin, K.-H., Hur, J., Lee, J.-S., Giesy, J.P., Khim, J.S., 2019. Newly Identified AhR-Active Compounds in the Sediments of an Industrial Area Using Effect-Directed Analysis. Environ. Sci. Technol. 53, 10043-10052.

Lee, J., Hong, S., Kim, T., Lee, C., An, S.-A., Kwon, B.-O., Lee, S., Moon, H.-B., Giesy, J.P., Khim, J.S., 2020. Multiple Bioassays and Targeted and Nontargeted Analyses to Characterize Potential Toxicological Effects Associated with Sediments of Masan Bay: Focusing on AhR-Mediated Potency. Environ. Sci. Technol. 54, 4443-4454.